ELSEVIER

Journal of Biomechanics ▮ (▮▮▮▮) ▮▮▮–▮▮▮

JOURNAL OF BIOMECHANICS

www.elsevier.com/locate/jbiomech
www.JBiomech.com

A new in vivo technique for determination of 3D kinematics and contact areas of the patello-femoral and tibio-femoral joint

R. von Eisenhart-Rothe[a,*], M. Siebert[b], C. Bringmann[b], T. Vogl[c], K.-H. Englmeier[b], H. Graichen[a]

[a] Department of Orthopedic Surgery, Research Group for Kinematics and Biomechanics, University of Frankfurt, Marienburgstr. 2, 60528 Frankfurt, Germany

[b] Institute for Medical Informatics, GSF Neuherberg, Ingolstädter Landstr. 1, 85764 Oberschleißheim, Germany

[c] Institute for Clinical and Interventional Radiology, University of Frankfurt, Theodor Stern Kai 7, 60590 Frankfurt, Germany

Accepted 29 September 2003

Abstract

Patello-femoral disorders are often caused by changes of patello-femoral and/or tibio-femoral kinematics. However, until now there has been no quantitative in vivo technique, that is able to obtain 3D kinematics and contact areas of all knee compartments simultaneously on a non-invasive basis. The aim of this study was therefore to develop and apply a technique which allows for determination of 3D kinematics and contact areas of the patello-femoral and tibio-femoral joint during different knee flexion angles and under neuromuscular activation patterns.

One knee of each of the 10 healthy volunteers was examined in an open MR system under flexing isometric muscle activity at 30° and 90°. Three-dimensional kinematics and contact areas of the patello-femoral and tibio-femoral joints were analyzed by 3D image postprocessing.

The reproducibility of the imaging technique yielded a coefficient of variation of 4.6% for patello-femoral, 4.7% for femoro-tibial displacement and 8.6% for contact areas. During knee flexion (30–90°), patella tilt (opened to medial) decreased ($8.8 \pm 3.4°$ vs. $4.6 \pm 3.1°$, $p < 0.05$), while lateral patellar shift increased significantly (1.6 ± 2.3 mm vs. 3.4 ± 3.0 mm, $p < 0.05$).

Furthermore, a significant posterior translation and external rotation of the femur relative to the tibia was observed. Patello-femoral contact areas increased significantly in size ($134 \pm 60\,mm^2$ vs. $205 \pm 96\,mm^2$) during knee flexion.

This technique shows a high reproducibility and provides physiologic in vivo data of 3D kinematics and contact areas of the patello-femoral and the tibio-femoral joint during knee flexion. This allows for advanced in vivo diagnostics, and may help to improve therapy of patello-femoral disorders in the future.

Keywords: Knee; Kinematics; Patella shift; Patella tilt; Open MR imaging; Contact areas

1. Introduction

Patello-femoral disorders are often attributed to malalignement and maltracking of the patella and occur in various pathologies of the knee joint (Hsieh et al., 2002; McNally, 2001). In total knee replacement, patello-femoral disorders are responsible for up to 50% of all revisions (Komistek et al., 2000; Lee et al., 1997). The reason for alteration in patellar kinematics is frequently not only located in the patello-femoral joint, but can also be caused by changes of tibio-femoral motion patterns. Different studies (Hsieh et al., 2002; Lee et al., 2001) using in vitro knee models have shown that in anterior cruciate ligament (ACL) insufficiency an increased anterior translation and valgus rotation of the tibia leads to lateral tilting and shifting of the patella. Until now, however, there has been no in vivo study to investigate patello-femoral and tibio-femoral kinematics simultaneously, though this seems essential for a better understanding of the complex knee joint biomechanics.

Recent in vivo analyses of patello-femoral kinematics have been performed using highfield MRI or cine MRI

*Corresponding author. Tel.: +49-69-6705-0; fax: +49-69-6705-375.

E-mail address: r_veisenhart@yahoo.de (R. von Eisenhart-Rothe).

0021-9290/$ - see front matter © 2003 Published by Elsevier Ltd.
doi:10.1016/j.jbiomech.2003.09.034

(Brossmann et al., 1993; Sheehan et al., 1999; Witonski and Goraj, 1999), all having their specific limitations. The standard highfield MRI analysis, for example, is usually restricted to two dimensions, potentially neglecting movements that deviate from the image plane (Closkey and Windsor, 2001; Lee et al., 1997). Furthermore, it is impossible to relocate an identical section plane and orientation in successive imaging sessions (Maganaris, 2000), which limits the use of these 2D techniques for intra- and inter-individual studies. Additionally, due to the construction of the MR scanner, the assessment can only be performed in knee flexion angles of less than 40° (Brossmann et al., 1993; Witonski and Goraj, 1999). Though it has been demonstrated that in different patello-femoral disorders, the symptoms occur especially in greater flexion angles (Tanzer et al., 2001; Witonski and Goraj, 1999).

Patello-femoral contact areas were shown to shift and decrease in patients with altered patellar kinematics (Hsieh et al., 2002; Huberti and Hayes, 1984; Kuroda et al., 2001), leading to increased contact pressure and the potential damage of the articular cartilage (Cohen et al., 1999; Huberti and Hayes, 1984). Therefore, simultaneous investigation of patellar kinematics and identification of potentially altered patello-femoral contact areas would be clinically relevant. However, until now, measurements of either tibio-femoral or patello-femoral contact patterns have mainly been performed in vitro (Ficat and Hungerford, 1977; Fukubayashi and Kurosawa, 1980; Hsieh et al., 2002; Huberti and Hayes, 1984; Kuroda et al., 2001), except for the study performed by Cohen et al. (1999).

The objective of this study was to develop an in vivo technique which allows for simultaneous determination of 3D kinematics and contact areas of the patello-femoral and tibio-femoral joint during various degrees of knee flexion angles and under the influence of physiologic neuromuscular activation patterns. Prior to investigating pathological knee kinematics, data on physiological kinematics should be obtained.

2. Methods

The knee joints of 10 healthy volunteers (aged 18–36 years; 7 of which were male and 3 female) were examined. None of the volunteer's knees had any history of pain or injury. Highfield MR imaging performed prior to the study showed no degenerative cartilage alterations, ligament insufficiency, patella dysplasia or lateralization in the knee joints.

Kinematic analysis was performed in an open MR system (0.2 T; Magnetom-Open, Siemens, Erlangen, Germany) using a T1 weighted 3D gradient echosequence (TR 16.1 ms, TE 7.0 ms, flip angle 30°). Image acquisition was performed in sagittal orientation (slice

Fig. 1. Photograph showing a patient lying on his side on the MR open table. The positioning device allows for reproducible alignment of the knee flexion angle, and avoids motion artifacts during image acquisition. An external load of 3 kg, leading to a torque of about 10 Nm about the knee joint, is applied to the distal shank.

thickness: 1.875 mm) while constant orientation of the patella relative to the sagittal plane was ensured by a localizer-sequence performed prior to the 3D image acquisition. Acquisition time was 4 min 26 s, and in-plane resolution was 0.86 mm. The volunteers were placed on their side and the knee flexion angle (30° and 90°) was controlled by a special positioning device (Siemens, Erlangen, Germany; Fig. 1). This device does not interfere with MR image acquisition and allows for a reproducible alignment of different knee flexion angles while avoiding motion artifacts during imaging. Tibial rotation and translation were not affected by the positioning device. In both positions (30° and 90°), a weight of 3 kg was applied to the lower third of the shank (35 cm distal to the knee joint space), to produce a torque of 10 Nm. This torque was initiated in an extending direction which led to isometric activation of the flexors. The torque was applied in the leg plane perpendicular to the axis of the tibia using a nylon rope and pulley. Isometric muscle activity over the entire acquisition period was verified by surface electromyography of the flexor muscles which showed continuous, isolated activity. All parts of the study were approved by the local ethic committee, and written informed consent was obtained from all volunteers prior to MR imaging.

2.1. Digital image processing

After image acquisition, the data were transferred to a parallel computing system (Octane Duo, Silicon Graphics, Mountain View, CA, USA). The semi-automated segmentation of patella, femur and tibia was performed based on a gray-value oriented region-growing algorithm (Haubner et al., 1997). Segmentation time for each MR data set was approximately 45 min. After trilinear interpolation, all anatomic structures were reconstructed three-dimensionally.

For analysis of patello-femoral kinematics, a patella-based local coordinate system (PBCS) was calculated (Figs. 2–4), which allows determination of the position of the patella relative to the tibia and femur, and the amount and direction of displacement between the different flexion angles. Therefore the patella was segmented on a slice by slice basis and the centroid—being the center of a 3D object—was computed, based on the interpolated segmented voxel data (Figs. 2 and 3). The centroid defines the origin of the PBCS. Due to the shape of the patella, which has an almost identical expansion in the vertical and the transversal plane, the principal axis of the PBCS cannot be calculated reproducibly using principal axis decomposition. Therefore, the axes of the PBCS were determined as follows: the first axis $\vec{S}$ (sagittal orientation, Figs. 2 and 4) was defined as the sum of the first eigenvectors in each slice, whereas each eigenvector was weighted with the number of segmented pixels in the specific slice. The second axis $\vec{T}$ (Figs. 3 and 4) was in a first step calculated in the same way for the transversal plane which defines a vector $\vec{t}$. To create a coordinate system with perpendicular axes, this vector $\vec{t}$ was then orientated to be perpendicular to $\vec{S}$ without changing the plane defined by $\vec{t}$ and the y-axis (eigenvector $\vec{n}_E$) ($\vec{T} = \vec{S} \times \vec{n}_E$) :

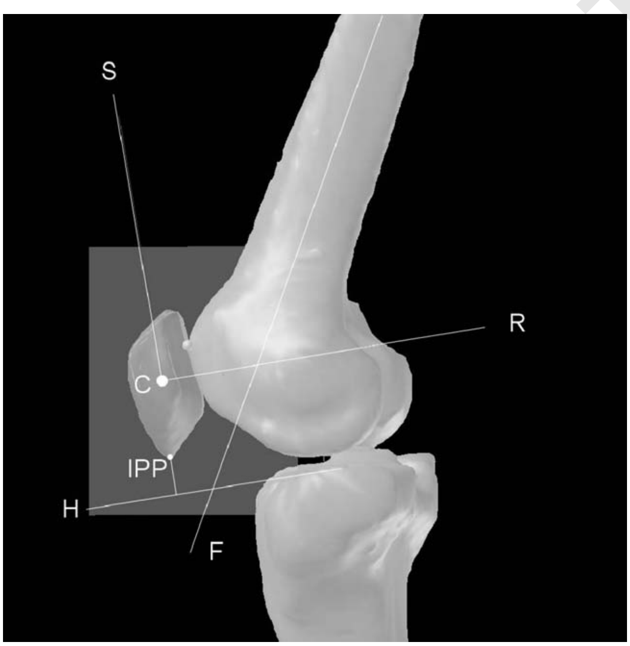

Fig. 2. Patellar-based coordinate system (sagittal view). C: centroid; S: first axis; R: third axis; H: second eigenvector of the tibia plateau; F: first eigenvector of the femur; IPP: inferior patella pole. Patello-femoral angle: angle between S and F; patellar height: distance between IPP and H.

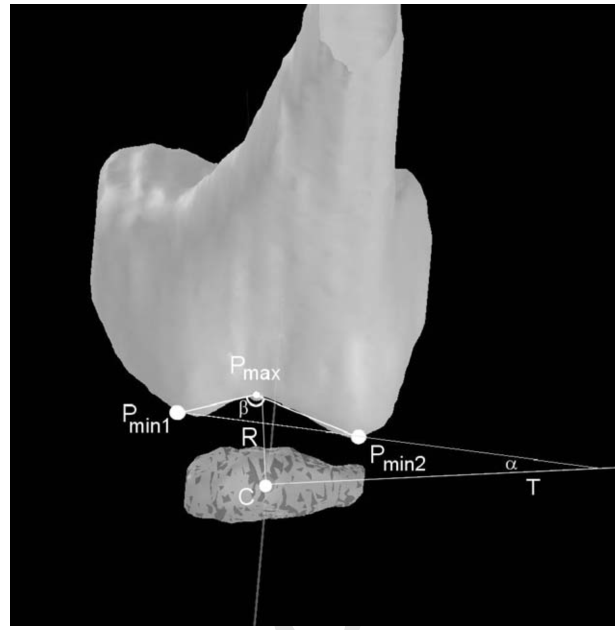

Fig. 3. Patellar-based coordinate system (transversal view). T: second axis ; R: third axis; P_{min1} and P_{min2}: shortest distance to the y–z-plane ($x=0$); P_{max}: largest distance to the y–z-plane ($x=0$). Sulcus angle β: angle between the line defined by P_{max}, P_{min1} and P_{min2}; tilt angle α: angle between the line defined by P_{min1} and P_{min2} and the second patella axis; +values: opened to medial; patellar shift: displacement between C and P_{max}, projected on T; +values: to lateral.

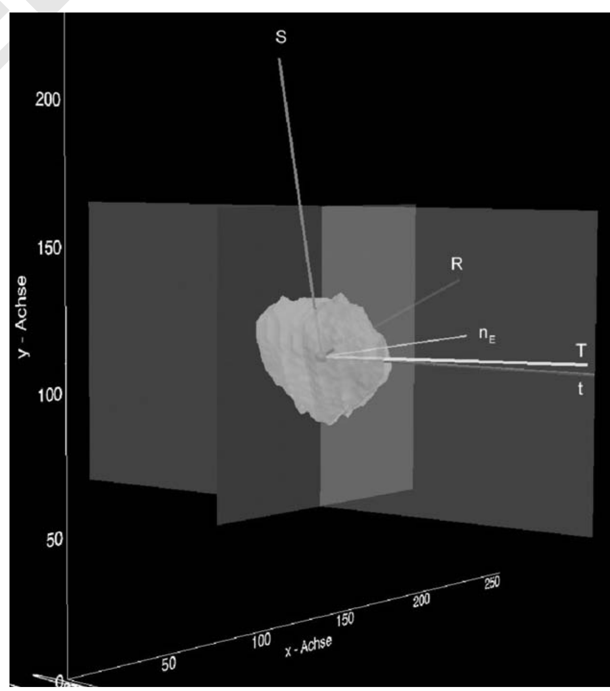

Fig. 4. Principal axis determination of the patellar-based coordinate system. $\vec{S}$: first axis superior–inferior orientation; $\vec{T}$: second axis medial–lateral orientation ($\vec{T} = \vec{S} \times \vec{n}_E$); $\vec{t}$: sum of the transversal eigenvectors in each slice, weighted with the number of segmented pixels in the specific slice; $\vec{n}_E$:eigenvector of the plane defined by $\vec{t}$- and y-axis; $\vec{R}$: third axis anterior–posterior orientation ($\vec{R} = \vec{S} \times \vec{T}$).

$$\vec{t} = \begin{pmatrix} t_1 \\ t_2 \\ t_3 \end{pmatrix} \quad (t_2 = 0,\ \text{because}\ \ \vec{t}\ \text{lays in the transversal plane}),$$

$$\vec{n}_E = \begin{pmatrix} 0 \\ 1 \\ 0 \end{pmatrix} \times \vec{t}$$

$$\vec{S} = \begin{pmatrix} s_1 \\ s_2 \\ 0 \end{pmatrix} \quad (s_3 = 0,\ \text{because}\ \ \vec{S}\ \text{lays in the sagittal plane}),$$

$$\vec{T} = \vec{S} \times \left(\begin{pmatrix} 0 \\ 1 \\ 0 \end{pmatrix} \times \begin{pmatrix} t_1 \\ 0 \\ t_3 \end{pmatrix} \right) \Rightarrow \vec{T} = \vec{S} \times \begin{pmatrix} t_3 \\ 0 \\ -t_1 \end{pmatrix} \Rightarrow \vec{T} = \begin{pmatrix} s_1 \\ s_2 \\ 0 \end{pmatrix} \times \begin{pmatrix} t_3 \\ 0 \\ -t_1 \end{pmatrix} = \begin{pmatrix} -s_2 t_1 \\ s_1 t_1 \\ -s_2 t_3 \end{pmatrix}.$$

The third axis $\vec{R}$ was then calculated perpendicular to $\vec{S}$ and $\vec{T}(\vec{R} = \vec{S} \times \vec{T})$.

Femoral reference points were also defined three-dimensionally in order to quantify the orientation and position of the patella relative to the femoral trochlear groove. Principal axis decomposition was used to determine the first eigenvector of the segmented femur. In the next step, for the lateral and medial femoral condyle, those points of the anterior part of the condyle were determined by which had the shortest distance to the y–z-plane ($x = 0$) (P_{min1} and P_{min2}; Fig. 3). In the trochlear groove the point with the largest distance to the y–z-plane ($x = 0$) was calculated (P_{max}; Fig. 3).

A tibia-based local coordinate system was calculated to determine the position of the patella and femoral condyles, the amount and direction of displacement between the different image acquisitions. To this end, the articular surface of the tibia plateau was segmented interactively in each slice, and the (area)-centroid of the tibia plateau was computed. Based on its spatial orientation, a 3D local coordinate system was determined, with its origin in the (area) centroid of the tibia plateau (Figs. 2 and 5).

Finally, the position of the reference points of the femur and tibia were projected in the PBCS. This allowed for a 3D determination of the established 2D parameters for describing patello-femoral kinematics (Gerber and Maenza, 1998; Lee et al., 1997; McNally, 2001; Witonski and Goraj, 1999) (Table 1).

To quantify tibio-femoral displacement, femoral reference points were defined which remain unaffected by knee flexion. Therefore, a cylinder fitting technique was applied to determine the epicondylar axis as described previously (von Eisenhart-Rothe et al., 2003). The position of the epicondylar axis was projected in the tibia-based coordinate system, which allows for determination of 3D position of the femur relative to the tibia (Fig. 5).

Fig. 5. Transepicondylar line of the femur defined by the center points of the constructed semi-cylinders for the lateral and medial femoral condyle. This reference system was used to determine the position and translation of the femur relative to the tibia in three dimensions.

To analyze the femoro-tibial and femoro-patellar contact areas, cartilage structures (femoral, tibial and patellar) were segmented in each slice. In slices with contact between femoral and tibial or patellar cartilage the two structures were separated by a line with the thickness of one pixel, so that each cartilage could be saved as separate data volumes. To calculate the contact areas the outline of each segmented cartilage was expanded by one pixel. All voxels that were segmented in both the femoral and tibial or patellar data volume were then counted. These voxels represent the contact areas.

To test reproducibility of the MR imaging and postprocessing technique, image acquisition of the same knee joint was performed 6 times (with 30° of flexion), segmentation and all postprocessing steps were performed on the 6 data sets by 1 observer. The measured parameters obtained during the different flexion angles were compared statistically using the Mann Whitney-U test (Statview 4.5, Abacus Concepts, Berkley, CA, USA).

Table 1
Measured parameters to describe patellar kinematics

3D sulcus angle	Angle between the line defined by P_{max}, P_{min1} and P_{min2} of the femur
Parameter in the sagittal plane	
Patello-femoral angle	Angle between first eigenvector of the segmented femur and first patellar axis *S*, projected in the sagittal plane.
Patellar height	Distance of the inferior patellar pole relative to the tibia plateau (tibia's second eigenvector), projected in the sagittal plane
Parameter in the transversal plane	
2D sulcus angle	Angle between the line defined by P_{max}, P_{min1} and $P_{min2}$of the femur; whereas the points have to be in the transversal patellar plane
Patellar shift	Displacement between the center of mass of the patella and P_{max}, projected on the second patellar axis. + values: to lateral
Tilt angle (relative to the anterior condylar line)	Angle between the line defined by P_{min1} and P_{min2} and the second patella axis, projected in the transversal patellar plane (+values: opened to medial)

Table 2
Reproducibility (mean values, standard deviation (SD) and coefficient of variation (COV) of the determined parameters to describe patello-femoral kinematics

	Sagittal plane			Transversal plane		
	Patellar height (mm)	Patello-femoral angle (°)	Sulcus-angle (2D) (°)	Sulcus-angle (3D) (°)	Tilt-angle (°)	Patellar shift (to lateral) (mm)
Mean	13.11	53.04	139.54	123.68	6.93	5.62
SD	0.61	3.16	1.71	2.03	0.50	0.47
COV	4.65	5.96	1.23	1.64	7.19	8.34

3. Results

3.1. Reproducibility of the image postprocessing technique

Reproducibility of the measured parameters for the patella kinematics yielded a coefficient of variation (CV%) of between 1.2% and 8.3% (Table 2). The femoro-tibial displacement mediolaterally (transepicondylar axis, medial/lateral reference points) also showed a high reproducibility with a standard deviation of 0.12 mm and a CV% of 4.7%. The values of displacement measured in this study exceeded the precision errors by a factor of 20:1.

For contact areas, the standard deviation was slightly higher with values of 6.2 mm^2 (mean: 73.8 mm^2) for the patello-femoral and 6.5 mm^2 (mean: 74.2 mm^2) for the tibio-femoral contact areas. The CV% was smaller than 9.0% (patello-femoral: 8.3%; tibio-femoral: 8.6%).

3.2. Effect of knee flexion (30°–90°) on knee kinematics

In the transversal plane, the patellar tilt (opened to medial) averaged 8.8°±3.4° at 30° of flexion. During knee flexion (30°–90°) tilting significantly decreased in all investigated knees ($p<0.05$, Table 3) whereas lateral patellar shift increased ($p<0.05$; Table 3). While the 3D sulcus angle for each individual stayed almost constant in both positions, the 2D angle (in the transversal patellar plane) decreased during knee flexion ($p=0.075$, Table 3). In the sagittal plane, the patello-femoral angle and the distance between the tibia plateau and the inferior part of the patella (patellar height) enlarged significantly ($p<0.05$) during knee flexion (Table 3).

During knee flexion (30°–90°), a significant ($p<0.05$) posterior translation of the femur relative to the tibia was observed (Table 4). Due to the additional external rotation of the transepicondylar line (Table 4) the amount of translation was higher for the lateral condyle. In the frontal plane, the angle of the transepicondylar line relative to the tibia plateau remained constant with values below 3°.

3.3. Effect of knee flexion (30°–90°) on the contact areas

At 30° of knee flexion, the femoro-patellar contact areas were located in the inferior part of the patellar articular cartilage. The contact was distributed across both patella facets, showing a broad transverse band (from medial to lateral; Fig. 6). The average size of the contact areas was 134.5±60.5 mm^2. At 90° of flexion,

Table 3
Parameters to describe patello-femoral kinematics (mean values and standard deviation)

	Sagittal plane			Transversal plane		
	Patellar height (mm)	Patello-femoral angle (°)	Sulcus-angle (2D) (°)	Sulcus-angle (3D) (°)	Tilt-angle (°)	Patellar shift (to lateral) (mm)
30° of flexion	15.7 ± 5.0	16.2 ± 9.1	145.2 ± 6.3	139.4 ± 6.5	8.8 ± 3.4	1.4 ± 1.9
90° of flexion	19.8 ± 4.1*	49.9 ± 6.3*	138.7 ± 9.0	138.3 ± 8.6	4.6 ± 3.1*	3.6 ± 3.2*

* = Significant ($p < 0.05$) difference 90° compared to 30° of knee flexion.

Table 4
Mean position and standard deviation of the femoral condyles (mm) and rotation of the transepicondylar line (°) relative to the tibia coordinate system (− = dorsal of the origin; + = internal rotation)

	Position		Translation
	30° flexion	90° flexion	(30°–90° flexion)
Central femur	−0.5 ± 2.1 mm	−1.7 ± 1.4* mm	1.2 ± 2.6 mm
Medial fem. condyle	−3.2 ± 2.0 mm	−2.4 ± 1.5 mm	−0.9 ± 2.9 mm
Lateral fem. condyle	2.2 ± 3.0 mm	−1.4 ± 3.3* mm	3.5 ± 3.6 mm
Femur rotation	6.2° ± 3.2°	1.2° ± 5.3°*	4.9° ± 3.9°

Central femur: midpoint of the epicondylar line; femur rotation: orientation of the epicondylar line relative to the first principal axis (x-axis) of the tibia coordinate system (medial–lateral); translation: mean translation (mm) from anterior to posterior during knee flexion (30°–90°).

* = Significant ($p < 0.05$) difference in position during 90° compared to 30° knee flexion.

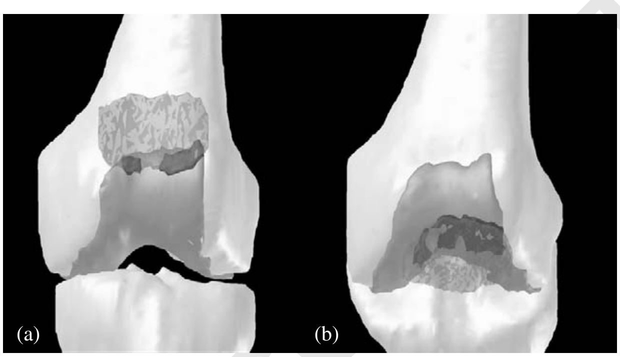

Fig. 6. Patello-femoral contact areas: (a) 30° of knee flexion and (b) 90° of knee flexion.

the contact areas migrated superiorly, the distribution still being a broad transversal band. The size of the contact areas increased significantly compared to 30° of flexion with a mean value of $205.4 \pm 96.6\,\mathrm{mm}^2$ ($p < 0.05$).

At 30° of knee flexion tibio-femoral contact was observed in both the medial and lateral compartment (Fig. 7), whereas in all knees the medial contact area was larger than the lateral. The contact was found to be in the central part of the lateral and medial tibia articular cartilage since the menisci were not segmented (Fig. 7). The lateral, anterior and posterior border of the tibial

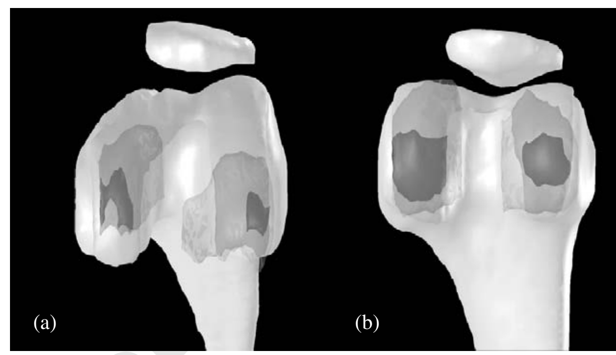

Fig. 7. Tibio-femoral contact areas: (a) 30° of knee flexion and (b) 90° of knee flexion.

articular cartilage therefore demonstrated no contact. The average size of the contact areas was $78.3 \pm 16.4\,\mathrm{mm}^2$. During knee flexion the contact areas shifted to the posterior aspect of the femoral condyles (Fig. 7) and size significantly increased ($122.8 \pm 17.3\,\mathrm{mm}^2$; $p < 0.05$).

4. Discussion

In this study, we have developed and applied a 3D MR-based imaging and postprocessing technique which allows for simultaneous in vivo assessment of tibio-femoral and patello-femoral 3D kinematics and contact areas. The results demonstrate that this method is highly reproducible for image acquisition and postprocessing. Healthy knees showed a significant decrease of the patellar tilt angle (opened to medial) during knee flexion (30°–90°), while lateral patellar shift increased significantly. In the sagittal plane, the femoro-patellar angle and the distance between the tibia plateau and the inferior part of the patella increased significantly. Regarding femoro-tibial displacement, posterior translation and external rotation of the femur relative to the tibia was observed during knee flexion. The contact area between femur and patella was located in the inferior part of the patellar articular cartilage at 30° and migrated superiorly during knee flexion. The average size of the contact areas increased significantly during knee flexion. This in vivo technique and the results stated previously allow for an advanced insight into the complex 3D kinematics of the knee joint, and may help to improve diagnostics and treatment of patello-femoral disorders.

Various studies have shown that conventional radiography is not capable of analyzing complex kinematics of the patella and therefore fails to exactly identify malalignement or maltracking (Brossmann et al., 1993; Ficat and Hungerford, 1977; Laurin et al., 1978). Recent in vivo analyses performed with 2D highfield MRI or CT (Muhle et al., 1999; Pinar et al., 1994; Schutze et al., 1986; Ward et al., 2002), suffered from limited reproducibility and restriction to two planes. Therefore, different authors (Closkey and Windsor, 2001; Heegaard et al., 2001; Lee et al., 1997) have mentioned the necessity of a 3D analysis. An additional limitation, caused by the closed construction of highfield MR-scanners, is that assessment can only be performed between 0° and 40° and not through the entire range of flexion (Brossmann et al., 1993; Sheehan et al., 1999; Witonski and Goraj, 1999). Open MRI, on the other hand, allows for the investigation of knee kinematics throughout the entire range of motion (Schmid et al., 2002; Steiner et al., 2001;) and by applying subsequent 3D postprocessing techniques three-dimensional quantification of all parameters is feasible. Additionally, by applying external forces during imaging, the effect of physiologic neuromuscular control patterns can be investigated.

To improve the reproducibility of previous interactive biomechanical analyses, determination of all reference points and other morphometric parameters was performed as fully automatic in this study. This, in contrast to previous cine MRI studies (Sheehan et al., 1999), in which the reference points were defined interactively, allowing variation reasoned by subjective interpretation (Sheehan et al., 1999). For patellar kinematics, a patella-based coordinate system and for femoro-tibial translation, a 3D transepicondylar axis technique was established. This postprocessing technique demonstrated a reproducibility which was considerably higher when compared to recent studies (Todo et al., 1999). Reproducibility of the contact areas was somewhat lower with a coefficient of variation of about 8.5%. This can be explained by the limited image resolution of the applied MR sequence (pixel size 0.86 mm). However, it is now feasible for the first time to assess contact patterns and calculate the approximate size of the contact areas in vivo and during isometric muscular activation throughout the entire range of motion.

One limitation of this technique—in contrast to cine MRI—is that assessment is limited to static loading conditions. To obtain complete 3D MR data sets, imaging times of approx. 3–5 min are required. Currently dynamic studies can only be performed with single 2D images, thus dealing with the problem of a limited reproducibility.

In accordance with our findings, Lee et al. (1997) reported on a patello-femoral angle in the sagittal plane of approximately 22° at 30° of flexion increasing to approximately 60° at 90° of knee flexion. Our results for patellar shifting and tilting also agree with previous data (Lee et al., 1997; Mizuno et al., 2001; Witonski and Goraj, 1999). The 3D sulcus angle measured in this study remained unchanged, which supports the high reproducibility of this technique. The 2D angle (in the patellar transversal plane), on the other hand, decreased during knee flexion, which is in good agreement with the findings of Tennant et al. (2001).

The results for the patello-femoral contact areas were also in conformity with those of previous investigations. Cohen et al. (1999) in a highfield MRI study also demonstrated a medial to lateral orientated contact area between the distal region of the retropatellar surface and the proximal portion of the trochlear groove at 30° of knee flexion. In vitro studies (Ficat and Hungerford, 1977; Hsieh et al., 2002; Huberti and Hayes, 1984; Tanzer et al., 2001) reported on medio-lateral contact areas, migrating from the distal third to the proximal margin of the retropatellar surface during knee flexion. Hsieh et al. (2002) reported on a total contact area of 138 mm^2 at 30° of knee flexion increasing to a size of 328 mm^2 at 90° using fuji prescale, which is in good agreement with our findings. For the tibio-femoral contact areas our results were also in good conformity with previous studies (Fukubayashi and Kurosawa, 1980; Kettelkamp and Jacobs, 1972; Walker and Erkman, 1975). In accordance to our findings Walker and Erkman (1975) and Fukubayashi and Kurosawa (1980) reported that contact was distributed about both condyles, whereas the medial side demonstrated a larger contact area than the lateral. Fukubayashi and Kurosawa (1980) found that the contact was mainly located on the menisci. As we did not segment the menisci, the size of the contact areas measured in the present study are comparable with those after removal of the menisci at about 200 N load (Fukubayashi and Kurosawa, 1980). However, direct comparison of both techniques is difficult since the in vitro values were obtained with the knee in full extension.

In conclusion, we have developed and applied a 3D MR-based imaging and postprocessing technique to determine patello-femoral and tibio-femoral translation patterns and contact areas in vivo. It could be shown that the technique has a high reproducibility which makes it feasible to investigate the entire knee kinematics simultaneously. In the future it can be used to improve diagnostics and the advance treatment of femoro-patellar disorders.

Acknowledgements

We would like to express our gratitude to the Deutsche Forschungsgemeinschaft (DFG; GR 1638/5-1, 5-2), the Klein Foundation and Alpha-Norm Medizintechnik GmbH for their support. The results of this study are part of the doctoral thesis of Christoph Bringmann, which will be submitted to the Ludwig-Maximilians University, Munich.

References

Brossmann, J., Muhle, C., Schroder, C., Melchert, U.H., Bull, C.C., Spielmann, R.P., Heller, M., 1993. Patellar tracking patterns during active and passive knee extension: evaluation with motion-triggered cine MR imaging. Radiology 187, 205–212.

Closkey, R.F., Windsor, R.E., 2001. Alterations in the patella after a high tibial or distal femoral osteotomy. Clinical Orthopaedics 389, 51–56.

Cohen, Z.A., McCarthy, D.M., Kwak, S.D., Legrand, P., Fogarasi, F., Ciaccio, E.J., Ateshian, G.A., 1999. Knee cartilage topography, thickness, and contact areas from MRI: in vitro calibration and in vivo measurements. Osteoarthritis and Cartilage 7, 95–109.

Ficat, R.P., Hungerford, D.S., 1977. Disorders of the Patellofemoral Joint. Williams & Wilkins, Baltimore, MD, pp. 85–109.

Fukubayashi, T., Kurosawa, H., 1980. The contact area and pressure distribution pattern of the knee. Acta Orthopaedica Scandinavica 51, 871–879.

Gerber, B.E., Maenza, F., 1998. Shift and tilt of the bony patella in total knee replacement. Der Orthopaede 27, 629–636.

Haubner, M., Eckstein, F., Lösch, A., Schnier, M., Sittek, H., Becker, C., Kolem, H., Reiser, M., Englmeier, K.-H., 1997. A non-invasive technique for 3-dimensional assessment of articular cartilage thickness based on MRI-part II: validation with CT arthrography. Magnetic Resonance Imaging 15, 805–813.

Heegaard, J.H., Leyvraz, P.F., Hovey, C.B., 2001. A computer model to simulate patellar biomechanics following total knee replacement: the effects of femoral component alignment. Clinical Biomechanics 16, 415–423.

Hsieh, Y.F., Draganich, L.F., Ho, S.H., Reider, B., 2002. The effects of removal and reconstruction of the anterior cruciate ligament on the contact characteristics of the patellofemoral joint. American Journal of Sports Medicine 30, 121–127.

Huberti, H.H., Hayes, W.C., 1984. Patellofemoral contact pressure–the influence of Q-angle and tendofemoral contact. Journal of Bone and Joint Surgery A66, 715–724.

Kettelkamp, D., Jacobs, A.W., 1972. Tibiofemoral contact area-determination and implications. Journal of Bone and Joint Surgery B54, 349–356.

Komistek, R.D., Dennis, D.A., Mabe, J.A., Walker, S.A., 2000. An in vivo determination of patellofemoral contact positions. Clinical Biomechanics 15, 29–36.

Kuroda, R., Kambic, H., Valdevit, A., Andrish, J.T., 2001. Articular cartilage contact pressure after tibial tuberosity transfer. A cadaveric study. American Journal of Sports Medicine 29, 403–409.

Laurin, C.A., Levesque, H.P., Dussault, R., Labelle, H., Peides, J.P., 1978. The abnormal lateral patellofemoral angle: a diagnostic roentgenographic sign of recurrent patellar subluxation. Journal of Bone and Joint Surgery A60, 55–60.

Lee, T.Q., Gerken, A.P., Glaser, F.E., Kim, W.C., Anzel, S.H., 1997. Patellofemoral joint kinematics and contact pressures in total knee arthroplasty. Clinical Orthopaedics 340, 257–266.

Lee, T.Q., Yang, B.Y., Sandusky, M.D., McMahon, P.J., 2001. The effects of tibial rotation on the patellofemoral joint: assessment of the changes in situ strain in the peripatellar retinaculum and the patellofemoral contact pressures and areas. Journal of Rehabilitation Research and Development 38, 463–469.

Maganaris, C.N., 2000. In vivo measurement-based estimations of the moment arm in the human tibialis anterior muscle-tendon unit. Journal of Biomechanics 33, 375–379.

McNally, E.G., 2001. Imaging assessment of anterior knee pain and patellar maltracking. Skeletal Radiology 30, 484–495.

Mizuno, Y., Kumagai, M., Mattessich, S.M., Elias, J.J., Ramrattan, N., Cosgarea, A.J., Chao, E.Y., 2001. Q-angle influences tibiofemoral and patellofemoral kinematics. Journal of Orthopaedic Research 19, 834–840.

Muhle, C., Brossmann, J., Heller, M., 1999. Kinematic CT and MR imaging of the patellofemoral joint. European Radiology 9, 508–518.

Pinar, H., Akseki, D., Karaoglan, O., Genc, I., 1994. Kinematic and dynamic axial computed tomography of the patello-femoral joint in patients with anterior knee pain. Knee Surgery, Sports Traumatology, Arthroscopy 2, 170–173.

Schmid, M.R., Hodler, J., Cathrein, P., Duewell, S., Jacob, H.A., Romero, J., 2002. Is impingement the cause of jumper's knee? Dynamic and static magnetic resonance imaging of patellar tendinitis in an open-configuration system. American Journal of Sports Medicine 30, 388–395.

Schutzer, S.F., Ramsby, G.R., Fulkerson, J.P., 1986. The evaluation of patellofemoral pain using computerized tomography. A preliminary study. Clinical Orthopaedics 204, 286–293.

Sheehan, F.T., Zajac, F.E., Drace, J.E., 1999. In vivo tracking of the human patella using cine phase contrast magnetic resonance imaging. Journal of Biomechanical Engineering 121, 650–656.

Steiner, M.E., Koskinen, S.K., Winalski, C.S., Martin, S.D., Haymen, M., 2001. Dynamic lateral patellar tilt in the anterior cruciate ligament-deficient knee. A magnetic resonance imaging analysis. American Journal of Sports Medicine 29, 593–599.

Tanzer, M., McLean, C.A., Laxer, E., Casey, J., Ahmed, A.M., 2001. Effect of femoral component designs on the contact and tracking characteristics of the unresurfaced patella in total knee arthroplasty. Canadian Journal of Surgery 44, 127–133.

Tennant, S., Williams, A., Vedi, V., Kinmont, C., Gedroyc, W., Hunt, D.M., 2001. Patello-femoral tracking in the weight-bearing knee: a study of asymptomatic volunteers utilising dynamic magnetic resonance imaging: a preliminary report. Knee Surgery, Sports Traumatology, Arthroscopy 9, 155–162.

Todo, S., Kadoya, Y., Moilanen, T., Kobayashi, A., Yamano, Y., Iwaki, H., Freeman, M.A., 1999. Anteroposterior and rotational movement of femur during knee flexion. Clinical Orthopaedics 362, 162–170.

von Eisenhart-Rothe, R., Siebert, M., Bringmann, C., Reiser, M., Englmeier, K.-H., Eckstein, F., Graichen, H. Differences between femoro-tibial and menisco-tibial translation patterns in patients with anterior cruciate ligament deficiency. A potential reason for secondary meniscal tears. Journal of Orthopaedic Research, accepted for publication.

Walker, P.S., Erkman, M.J., 1975. The role of the menisci in force transmission across the knee. Clinical Orthopaedics 106, 184–192.

Ward, S.R., Shellock, F.G., Terk, M.R., Salsich, G.B., Powers, C.M., 2002. Assessment of patellofemoral relationships using kinematic MRI: comparison between qualitative and quantitative methods. Journal of Magnetic Resonance Imaging 16, 69–74.

Witonski, D., Goraj, B., 1999. Patellar motion analyzed by kinematic and dynamic axial magnetic resonance imaging in patients with anterior knee pain syndrome. Archives of Orthopaedic and Trauma Surgery 119, 46–49.